

Measurement of cross sections and couplings of the SM Higgs boson in the ZZ^* decay channel using the ATLAS detector

Ludovica Aperio Bella^{*†}

University of Birmingham (new affiliation CERN)

E-mail: ludovica.aperio.bella@cern.ch

The Higgs boson decay to four leptons, $H \rightarrow ZZ^* \rightarrow 4\ell$, where $\ell = e$ or μ , provides good sensitivity for the measurement of its properties due to its high signal-to-background ratio (S/B), which is better than two for each of the four final states: 4μ , $2e2\mu$, $2\mu2e$ and $4e$, where the first lepton pair is defined to be the one with the dilepton invariant mass closest to the Z boson mass.

These proceedings summarise several preliminary results on the properties of the Higgs boson decaying to four leptons final state using 14.8 fb^{-1} of integrated luminosity collected in pp collisions by the ATLAS detector at the LHC at a centre-of-mass energy of 13 TeV [1]. The results include measurements of the fiducial cross sections, the different production mode cross sections and a test of beyond the Standard Model interactions using an effective Lagrangian approach.

38th International Conference on High Energy Physics
3-10 August 2016
Chicago, USA

^{*}Speaker.

[†]On behalf of the ATLAS collaboration



1. Introduction

The observation of a new particle compatible with the Standard Model (SM) Higgs boson by the ATLAS and CMS experiments [2, 3] based on the data from LHC Run1 taken during 2011 and 2012, has been an important step towards the clarification of the mechanism of the electroweak (EW) symmetry breaking.

These proceedings summarise several preliminary results on the properties of the Higgs boson decaying to the four lepton final state using 14.8 fb^{-1} of integrated luminosity collected in pp collisions by the ATLAS detector at the LHC at a centre-of-mass energy of 13 TeV [1]. The results include measurements of the fiducial cross sections, the different production-mode cross sections and a test of beyond the Standard Model interactions using an effective Lagrangian approach.

2. Event selection and signal region yields

Table 1: The numbers of events expected and observed for a $m_H=125 \text{ GeV}$ hypothesis for each of the four-lepton final states. The second column gives the expected signal without any cut on $m_{4\ell}$. The other columns give for the 118–129 GeV mass range, the numbers of expected signal events and of expected ZZ^* and other background events, the signal-to-background ratios (S/B), and the numbers of observed events, for 14.8 fb^{-1} at $\sqrt{s} = 13 \text{ TeV}$. The uncertainties include both the statistical and systematic components [1].

Final State	Signal	Signal	ZZ^*	other bkg.	S/B	Expected	Observed
	(full mass range)	(118 < $m_{4\ell}$ < 129 GeV)					
4μ	8.8 ± 0.6	8.2 ± 0.6	3.11 ± 0.30	0.31 ± 0.04	2.4	11.6 ± 0.7	16
$2e2\mu$	6.1 ± 0.4	5.5 ± 0.4	2.19 ± 0.21	0.30 ± 0.04	2.2	8.0 ± 0.4	12
$2\mu 2e$	4.8 ± 0.4	4.4 ± 0.4	1.39 ± 0.16	0.47 ± 0.05	2.3	6.2 ± 0.4	10
$4e$	4.8 ± 0.5	4.2 ± 0.4	1.46 ± 0.18	0.46 ± 0.05	2.2	6.1 ± 0.4	6
Total	24.5 ± 1.8	22.3 ± 1.6	8.2 ± 0.8	1.54 ± 0.18	2.3	32.0 ± 1.8	44

The ATLAS detector is described in detail elsewhere [4]. The reconstruction and identification of electrons, muons and jets, as well as the event selection follow closely the strategy described in Ref. [5]. Higgs boson candidates are formed by selecting two same-flavour, opposite-sign lepton pairs (a lepton quadruplet) in an event. Quadruplet selection is done separately in each sub-channel: 4μ , $2e2\mu$, $2\mu 2e$, $4e$. The kinematic selection applied to the leptons is the same as the one detailed in previous publications with a few small changes described in the following. In order to cope with the increase of the reducible background coming from heavy flavour decay, due to the lowering of the minimum muon p_T requirement (lowered from 6 to 5 GeV), the four leptons are required to be compatible with the same vertex. A loose χ^2 selection is applied, corresponding to a signal efficiency of 99.5% for all decay channels. For each channel, the same-flavour opposite-charge lepton pair with the mass closest (second closest) to the Z boson mass is referred to as the leading (subleading) dilepton and its invariant mass is referred to as m_{12} (m_{34}). Each lepton four-momentum vector is corrected for QED final state radiation, and the lepton four-momenta of the leading dilepton are recomputed by means of a Z -mass-constrained kinematic fit. The Z -mass constraint improves the

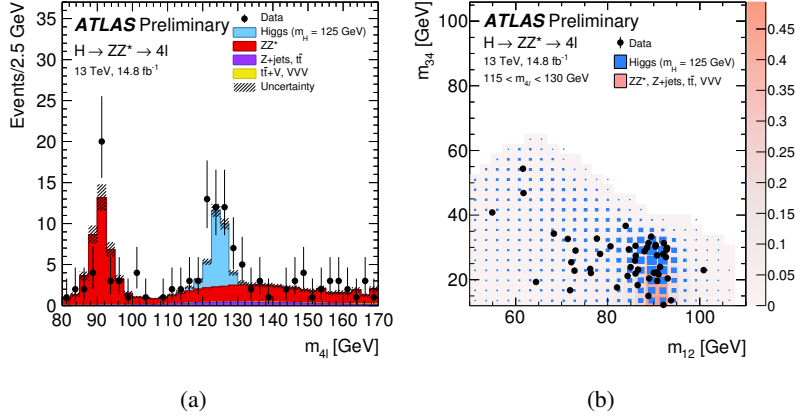


Figure 1: (a) The $m_{4\ell}$ distribution of the selected candidates, compared to the background expectation in the low mass region [1]. (b) The distribution of data (filled circles) and the expected signal and backgrounds events in the $m_{34} - m_{12}$ plane with the requirement of $m_{4\ell}$ in 115–130 GeV. The expected distributions of the Higgs signal (blue) and total background (red) are superimposed, where the box size (signal) and colour shading (background) represent the relative density [1].

$m_{4\ell}$ resolution by about 15%. Events satisfying the above criteria are considered candidate signal events. Two $m_{4\ell}$ ranges are defined and used as signal region in the following.

The production of the SM Higgs boson is modelled using the POWHEG-BOX Monte Carlo (MC) event generator interfaced to PYTHIA 8 for parton shower, hadronization, which calculates separately the ggF and VBF production mechanisms with matrix elements up to next-to-leading order (NLO) in QCD. PYTHIA 8 is used to simulate at LO in QCD, the production of a Higgs boson in association with a W or a Z boson, and the production of a Higgs boson in association with a top quark pair is simulated at NLO in QCD, using MADGRAPH5_AMC@NLO interfaced to HERWIG++ for showering and hadronization.

The main background contribution to the four lepton final state is from the non-resonant ZZ^* production which is modelled using simulation normalised to the SM predictions. The ZZ^* continuum background from quark-antiquark annihilation is modelled at NLO in QCD using POWHEG-BOX interfaced to PYTHIA 8. For the quark-initiated ZZ^* NNLO QCD and NLO EW corrections are applied as function of m_{ZZ^*} [6]. The gluon induced ZZ^* production is simulated using GG2VV. The k-factor accounting for higher order QCD effects for the $gg \rightarrow ZZ^*$ continuum production has been calculated including the $gg \rightarrow H^* \rightarrow ZZ$ processes [7]. Additional background sources are the Z +jets and $t\bar{t}$ processes, which are estimated in the signal region using different data-driven techniques according to the flavour of the sub-leading lepton pairs ($\mu\mu$ or ee), following the methods described in [5]. The background from WZ production is estimated from data for the $\ell\ell + ee$ final states, while it is taken from simulation for the $\ell\ell + \mu\mu$ final states. The contributions from $t\bar{t}V$ and triboson processes are minor and taken from POWHEG-BOX interfaced to PYTHIA 6 simulation.

The numbers of observed candidate events for each of the four decay channels in the mass window 118–129 GeV and the signal and background expectations are presented in Table 1.

The mass spectrum for $m_{4\ell}$ is shown for the selected events in Fig. 1(a) together with the expected

ZZ^* and reducible backgrounds, and an expected SM Higgs signal at 125 GeV. Figure 1(b) shows the distribution of m_{12} versus m_{34} for the candidates with $m_{4\ell}$ within 115–130 GeV.

3. Fiducial cross sections measurement

The selected events in the mass region $115 < m_{4\ell} < 130$ GeV are analyzed to extract the fiducial and total cross sections. In order to minimize the model dependence of the cross section measurement, the fiducial phase space defined in details in Ref. [1], follows closely the experimental requirements applied to the four leptons. The $m_{4\ell}$ distribution is used as a discriminant to increase the sensitivity to the signal through the definition of probability density functions (PDF) for the signal and the background in each four-lepton channel and for each production mode:

$$N_{Data}(m_{4\ell}) = \mathcal{L}_{int} \cdot \sigma^{\text{tot}} \cdot B(H \rightarrow 4\ell) \cdot PDF_{sig}(m_{4\ell}) \cdot \mathcal{A} \cdot \mathcal{C} + PDF_{bkg}(m_{4\ell}) \cdot N_{bkg} \quad (3.1)$$

where $N_{Data}(m_{4\ell})$ is the number of observed data candidates as a function of $m_{4\ell}$, \mathcal{L}_{int} the integrated luminosity, σ^{tot} is the total production cross section of the Higgs boson, $B(H \rightarrow 4\ell)$ is the branching ratio of the Higgs boson decay into the four lepton final state, \mathcal{A} is the acceptance factor in the fiducial region, \mathcal{C} is a detector correction factor, which account for effects such as trigger, reconstruction and identification efficiencies and for the resolution, and N_{bkg} is the number of estimated background events.

The fiducial cross sections are extracted with a likelihood fit to the observed $m_{4\ell}$ distribution in the signal mass window for each channel. The total fiducial cross section is obtained as the sum of the four final states, $\sigma_{\text{fid,sum}}^{4\ell} = 4.48_{-0.89}^{+1.01}$ fb. This value have to be compared with the expected SM value $\sigma_{\text{fid,SM}}^{4\ell} = 3.07_{-0.25}^{+0.21}$ fb.

The total cross section is obtained by extrapolating the $\sigma_{\text{fid}}^{4\ell}$ to the full phase-space using the fiducial acceptance factors \mathcal{A} assuming that the production mode cross-section ratios are the same as predicted by the SM and the SM branching ratio $\mathcal{B}(H \rightarrow 4\ell)$:

$$\sigma_{\text{tot}} = 81_{-16}^{+18} \text{ pb}, \quad (3.2)$$

to be compared with the expected SM value $\sigma_{\text{tot,SM}} = 55.5_{-4.4}^{+3.8}$ pb. The compatibility between the total measured cross section and the SM prediction is at the level of 1.6 standard deviations. In all the cross section measurements presented here the dominant uncertainty is statistical.

4. Cross sections per production mode from event categorisation

In order to improve the sensitivity to the different production modes, the events selected in the mass region $118 < m_{4\ell} < 129$ GeV are classified into exclusive categories. The narrower mass range gives better performance when the mass is not used as a discriminant in the fit. Categories based on the presence of additional leptons ($p_{T,l} > 8$ GeV) and the number of jets ($p_{T,jet} > 30$ GeV) are used with several multivariate discriminants (BDT) optimized to disentangle the different production modes. The number of expected and observed events in each of the categories, are summarized in Table 2.

The cross section for the different production modes are extracted through a likelihood fit to the BDT distribution in the different categories evaluated assuming $m_H=125.09$ GeV. The measured

Table 2: The expected and observed yields in the 0-jet, 1-jet, 2-jet with $m_{jj} > 120$ GeV (*VBF-enriched*), 2-jet with $m_{jj} < 120$ GeV (*VH-enriched*) and VH-leptonic categories. The yields are given for the different production modes (assuming $m_H = 125$ GeV), for the ZZ^* and the reducible backgrounds for 14.8 fb^{-1} at $\sqrt{s} = 13$ TeV. The estimates are given for the $m_{4\ell}$ mass range 118–129 GeV. The uncertainties include both the statistical and systematic components [1].

Analysis category	Signal				Background		Total expected	Observed
	ggF + $b\bar{b}H + t\bar{t}H$	VBF	WH	ZH	ZZ^*	Z + jets, $t\bar{t}$		
0-jet	11.2 ± 1.4	0.120 ± 0.019	0.047 ± 0.007	0.060 ± 0.006	6.2 ± 0.6	0.84 ± 0.12	18.4 ± 1.6	21
1-jet	5.7 ± 2.4	0.59 ± 0.05	0.137 ± 0.012	0.091 ± 0.008	1.62 ± 0.21	0.44 ± 0.07	8.5 ± 2.4	12
2-jet VBF enrich	1.9 ± 0.9	0.92 ± 0.07	0.074 ± 0.007	0.052 ± 0.005	0.22 ± 0.05	0.24 ± 0.11	3.4 ± 0.9	9
2-jet VH enrich	1.1 ± 0.5	0.084 ± 0.009	0.143 ± 0.012	0.101 ± 0.009	0.166 ± 0.035	0.088 ± 0.011	1.6 ± 0.5	2
VH-leptonic	0.055 ± 0.004	< 0.01	0.067 ± 0.004	0.011 ± 0.001	0.016 ± 0.002	0.012 ± 0.010	0.16 ± 0.01	0
Total	20 ± 4	1.71 ± 0.14	0.47 ± 0.04	0.315 ± 0.027	8.2 ± 0.9	1.62 ± 0.07	32 ± 4	44

values for the cross section in the different production categories with their SM expectations (on the right) are respectively:

$$\begin{aligned}
\sigma_{\text{ggF}+b\bar{b}H+t\bar{t}H} \cdot \mathcal{B}(H \rightarrow ZZ^*) &= 1.80^{+0.49}_{-0.44} \text{ pb} & \sigma_{\text{SM,ggF}+b\bar{b}H+t\bar{t}H} \cdot \mathcal{B}(H \rightarrow ZZ^*) &= 1.31 \pm 0.07 \text{ pb} \\
\sigma_{\text{VBF}} \cdot \mathcal{B}(H \rightarrow ZZ^*) &= 0.37^{+0.28}_{-0.21} \text{ pb} & \sigma_{\text{SM,VBF}} \cdot \mathcal{B}(H \rightarrow ZZ^*) &= 0.100 \pm 0.003 \text{ pb} \\
\sigma_{\text{VH}} \cdot \mathcal{B}(H \rightarrow ZZ^*) &= 0^{+0.15} \text{ pb} & \sigma_{\text{SM,VH}} \cdot \mathcal{B}(H \rightarrow ZZ^*) &= 0.059 \pm 0.002 \text{ pb}
\end{aligned} \tag{4.1}$$

The compatibility between the measured $\sigma_{\text{ggF}+b\bar{b}H+t\bar{t}H} \cdot \mathcal{B}(H \rightarrow ZZ^*)$ and the SM prediction is at the level of 1.1 standard deviations, while for the $\sigma_{\text{VBF}} \cdot \mathcal{B}(H \rightarrow ZZ^*)$ the compatibility with the SM prediction is at the level of 1.4 standard deviations. Figure 2(a) shows the negative log-likelihood contours in the $\sigma_{\text{ggF}+b\bar{b}H+t\bar{t}H} \cdot \mathcal{B}(H \rightarrow ZZ^*) - \sigma_{\text{VBF}+\text{VH}} \cdot \mathcal{B}(H \rightarrow ZZ^*)$ plane assuming that the production mode cross-section ratios are the same as predicted by the SM.

The experimental categorisation also provides sensitivity to possible BSM interactions. In particular, BSM interactions between the Higgs boson and the SM vector bosons W and Z would have a large impact on the yields in the VH and VBF production modes since they would modify simultaneously the production and the decay interactions. In order to study these interactions, effective Lagrangian terms related to the BSM scalar (κ_{HVV}) and pseudo-scalar (κ_{AVV}) interactions between the Higgs boson and the Z and W vector bosons are considered following the Higgs characterisation model described in Ref. [8]. Figures 2(b) and 2(c) show the expected and observed negative log-likelihood scans as function of the BSM coupling κ_{HVV} and $\kappa_{AVV} \cdot \sin \alpha$, derived with a fit of the yields in the categories, without exploiting any additional discriminant shape information. In each scan the other BSM coupling parameter is left free in the fit. As can be seen in Fig. 2(b), 2(c) the minima of the fits are not at $\kappa_{BSM} = 0$ and the observed exclusion limits are weaker than the expected limits. This is due to the fact that the observed number of events is larger than those predicted by the SM in several categories, in particular in the *2-jet VBF enriched* category. The agreement between $\kappa_{HVV} = 0$ and the observed value is 2.1 standard deviations and between $\kappa_{AVV} \cdot \sin \alpha = 0$ and the observed value is 1.8 standard deviations.

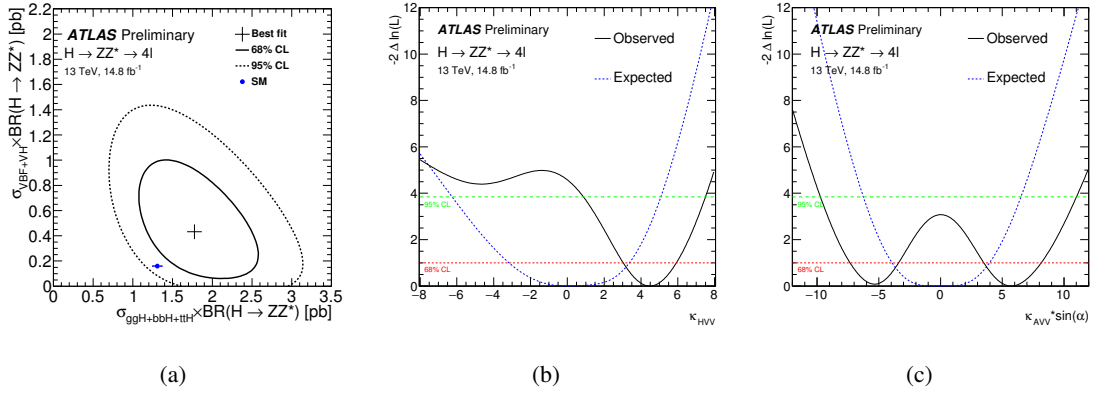


Figure 2: (a) Observed negative log-likelihood contours at 68% (solid line) and 95% CL (dashed line) in the $\sigma_{\text{ggF}+bbH+iH} \cdot \mathcal{B}(H \rightarrow ZZ^*) - \sigma_{\text{VBF}+VH} \cdot \mathcal{B}(H \rightarrow ZZ^*)$ plane together with the SM prediction (blue filled circle), with its theoretical uncertainty taken from Ref. [9]. The $\sigma_{\text{VBF}+VH} \cdot \mathcal{B}(H \rightarrow ZZ^*)$ is evaluated under the assumption that the relative contribution of these two production modes follows the SM prediction [1]. Observed negative log-likelihood scans (solid black line) for κ_{HVV} (b) and $\kappa_{AVV} \cdot \sin \alpha$ in (c) together with those expected for the SM Higgs boson (dashed blue line). The horizontal dashed lines indicate the value of the profile likelihood ratio corresponding to the 68% (red) and 95% (green) CL intervals for the parameter of interest, assuming the asymptotic χ^2 distribution of the test statistic [1].

5. Conclusions

The properties of the Higgs boson resonance have been studied in the four-lepton decay channel using 14.8 fb^{-1} of integrated luminosity collected in pp collisions by the ATLAS detector at the LHC at a centre-of-mass energy of 13 TeV. The measured properties are in agreement with SM predictions in terms of fiducial and total inclusive cross sections as well as in terms of cross sections per production mode. The categories used to measure the production mode cross sections have also been used to derive limits on possible BSM interactions of the Higgs boson with the SM vector bosons in the framework of an effective Lagrangian extension of the SM.

References

- [1] ATLAS Collaboration, [ATLAS-CONF-2016-079](#)
- [2] ATLAS Collaboration, *Phys. Lett. B*, 716, 1
- [3] CMS Collaboration, *Phys. Lett. B*, 716, 30
- [4] ATLAS Collaboration, *JINST* 3 2008, S08003
- [5] ATLAS Collaboration, [ATLAS-CONF-2015-059](#)
- [6] B. Biedermann et al., *Phys. Rev. Lett.* 116 (2016) 161803
- [7] C.S.Lietal., *JHEP* 08 (2015) 065
- [8] Artoisenet, P. and others, *JHEP* 11 (2013) 043
- [9] [Higgs Cross Section Working Group](#)